Experimental studies of the liquid-glass transition in trimethylheptane

G. Q. Shen,[1,*] J. Toulouse,[2] S. Beaufils,[3] B. Bonello,[4] Y. H. Hwang,[1,†] P. Finkel,[2,‡] J. Hernandez,[1,§] M. Bertault,[3] M. Maglione,[5] C. Ecolivet,[3] and H. Z. Cummins[1]

[1]*Department of Physics, City College of the City University of New York, New York, New York 10031*

[2]*Department of Physics, Lehigh University, 16A Sherman Fairchild Laboratory, Bethlehem, Pennsylvania 18015*

[3]*Groupe Matière Condensée et Matériaux, Université de Rennes I, Campus de Beaulieu, Bâtiment 11B, F-35042 Rennes Cedex, France*

[4]*Laboratoire des Milieux Désordonnés et Hétérogènes, Université Pierre et Marie Curie, Boîte Postale 86, 4 Place Jussieu, 75252 Paris Cedex 05, France*

[5]*Laboratoire de Physique, Université de Bourgogne Boîte Postale 400, F-21011 Dijon Cedex, France*

(Received 9 December 1999)

The molecular glass former trimethylheptane was studied by calorimetric, dielectric, ultrasonic, neutron scattering, Brillouin scattering, and depolarized light-scattering techniques. The molecular structure appears to be nearly spherical optically as indicated by the low depolarization ratio and dielectric susceptibility values. A preliminary mode-coupling theory (MCT) analysis of the light-scattering and neutron-scattering data indicates that $T_C \gtrsim 150$ K, at least 25 K above T_G. The susceptibility minima were analyzed with the MCT interpolation equation, and disagreement between the light and neutron results was observed despite the apparent isotropy of the molecules.

PACS number(s): 64.70.Pf, 78.35.+c, 61.12.−q

I. INTRODUCTION

Recent research on the liquid-glass transition has often relied on experimental data obtained with neutron- and light-scattering techniques. Interpretation of such data is usually based on theoretical predictions for the translational dynamics $S(q,\omega)$, but the spectra can also be affected by orientational dynamics (for molecular glass formers), or by chemical bonding rearrangements (for network glass formers). Thus there is considerable interest in identifying a fragile molecular glass-forming material free of both network and orientational effects that can serve as a model system for detailed tests of theories of the liquid-glass transition.

In 1984, Carroll and Patterson [1] reported Brillouin scattering experiments on a group of branched alkanes. One of the materials they studied, 2,4,6-trimethylheptane (TMH), was found to produce spectra with very low depolarization ratios, indicative of a molecular structure that is optically isotropic. Recently, a preliminary evaluation of the molecular conformation of TMH was carried out by Craig Brown at NIST with a program (CERIUS) that uses a simple interatomic model potential with fixed bond lengths and minimizes the total energy. The result, shown in Fig. 1, indicates a nearly globular conformation and supports the highly symmetric structure suggested by the low depolarization ratio observed in the light-scattering experiments.

Although TMH is commercially available, there is very little published experimental literature on its physical properties, apart from the Brillouin scattering study of Carroll and Patterson. We have therefore undertaken a series of studies of TMH with ultrasonics, light scattering, neutron scattering, differential scanning calorimetry, refractive index, and dielectric susceptibility techniques. In this publication, we present a preliminary report of the results obtained in these experiments.

II. EXPERIMENTS

A. Material properties

2,4,6-trimethylheptane ($C_{10}H_{22}$) of 99% stated purity was purchased from Wiley Organics (Coshocton, OH 43812) and, subsequently, from Chemsampco (Gray Court, SC 29645). For the light scattering, neutron scattering, and ultrasonics experiments it was distilled into glass sample cells

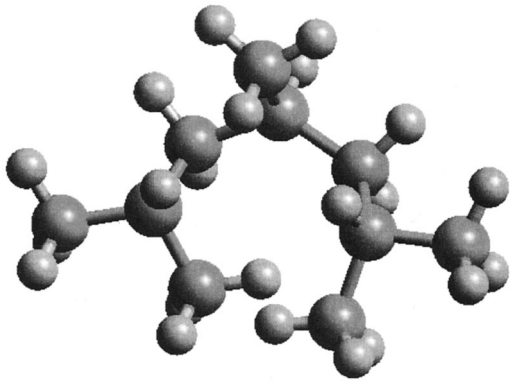

FIG. 1. Conformation of TMH predicted by CERIUS, a computer program that minimizes the total energy of the molecule with fixed bond lengths.

*Present address: Physics Department, Oklahoma State University, Stillwater, OK 74078.

†Present address: RCDAMP, Pusan National University, Pusan 609-735, Korea.

‡Present address: Physical Acoustics Corporation, P.O. Box 3135, Princeton, NJ 08543.

§Present address: Borough of Manhattan Community College, 199 Chambers St., New York, NY 10007.

 ©2000 The American Physical Society

TABLE I. Properties of 2,4,6-trimethylheptane (TMH).

Molecular weight, 142.28
$T_M = 219$ K
$T_B = 421$ K
$T_G = 125$ K
$T_C \approx 150$ K
$\rho(T) = 0.9568 - 7.946\times10^{-4}$ [T(K)] g/cm^3
$\eta(T) = 0.01514 \exp(1154/T)$ cP
$n_{488}(T) = 1.534 - 4.4\times10^{-4}$ T

and flame sealed under vacuum. For the other experiments it was used as provided by the supplier. Material properties of TMH supplied by the manufacturer are *molecular weight* $=142.28$, refractive index $n=1.4071$, specific gravity $=0.7225$. Yaws *et al.* [2] give the melting and boiling temperatures of TMH as $T_M = 219$ K, $T_B = 420.8$ K.

Carroll and Patterson [1] measured the density and viscosity of TMH as

$$\rho(T) = 0.9558 - 7.946\times10^{-4}[T(\mathrm{K})] \ \mathrm{g/cm^3}, \quad (1)$$

$$\eta(T) = 0.015\,14 \exp(1154/T) \ \mathrm{cP}. \quad (2)$$

(The temperature range in which these fits apply was not specified.)

We measured the refractive index $n(T)$ at 488 nm with the minimum deviation method using a triangular glass cuvette mounted in a cryostat. The result for the range 200–300 K was

$$n_{488}(T) = 1.534 - 4.4\times10^{-4}T. \quad (3)$$

These properties of TMH are summarized in Table I.

The specific heat C_P of TMH was measured at the Université de Rennes I by differential scanning calorimetry with a Perkin-Elmer Series 7 thermal analysis system. A scan at 10 K/min revealed a large jump in C_P centered at $T_G \sim 125$ K, from ~ 0.55 J/gK to ~ 1.1 J/gK as illustrated in Fig. 2. This same T_G was inferred by Carroll and Patterson from a change in slope of the Brillouin shift vs temperature plot.

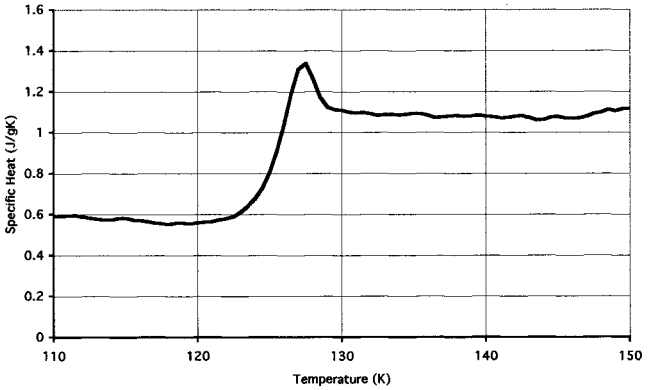

FIG. 2. Specific heat C_P of TMH measured by differential scanning calorimetry at 10 K/min. C_P increases from ~ 0.55 J/g K to ~ 1.1 J/g K in a step centered at $T_G \sim 125$ K.

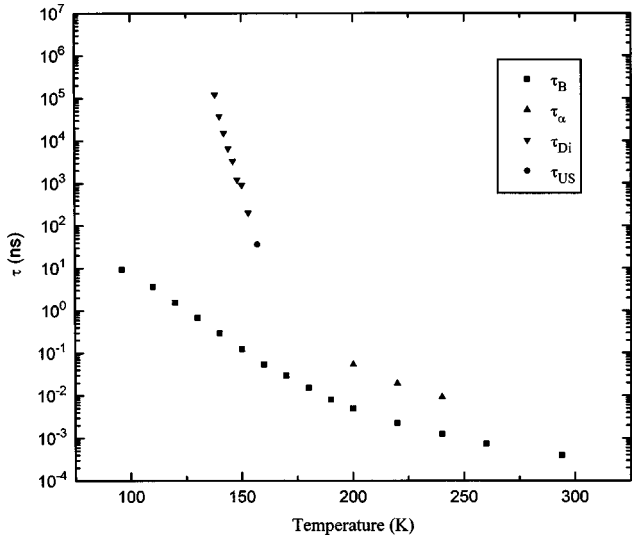

FIG. 3. Relaxation time of TMH obtained from Brillouin scattering analyzed with Mountain theory (■, τ_B), depolarized backscattering (▲, τ_α), and dielectric susceptibility analyzed with Cole-Davidson fits (▼, τ_{Di}). The single ultrasonic value at 157 K (●, τ_{US}) corresponds to $\omega\tau_{US}=1$ at the attenuation maximum, for $\omega/2\pi = 4.4$ MHz.

The viscosity measurements reported in Ref. [1] were fitted to the simple Arrhenius form shown in Eq. (2). No more extensive measurements of $\eta(T)$ are available, so the fragility of TMH has not been established. Nevertheless, for this preliminary study, we will assume that TMH is a simple van der Waals liquid, like most other molecular liquids, and that it is therefore relatively fragile.

B. Dielectric susceptibility

Dielectric measurements in the temperature range 100–298 K were carried out at the Université de Bourgogne in Dijon. Because of the highly symmetric structure of TMH, the signal was very weak (1.4 pF for the filled cell, 0.9 pF for the empty cell) corresponding to a permittivity of ~ 1.6, and measurements were only possible in the frequency range 10 kHz to 1 MHz.

Fits to $\epsilon'(\omega)$ were carried out for the temperature range 138–153 K with Debye, Cole-Cole, and Cole-Davidson functions with limited success due to the extremely weak signal. For $T<142$ K, the loss peak was not within the experimental window, and τ values were obtained from fits to the high-frequency part of $\epsilon'(\omega)$. The Cole-Davidson fits

$$\epsilon^*(\omega) = \epsilon_\infty + (\epsilon_S - \epsilon_\infty)/(1 - i\omega\tau)^\beta \quad (4)$$

with $\epsilon_\infty = 2.5718$, $\epsilon_S = 2.5954$, τ and β free, gave the τ values shown as τ_{Di} in Fig. 3, plotted together with τ values obtained from ultrasonics (τ_{US}), Brillouin scattering (τ_B), and depolarized backscattering experiments (τ_α) to be discussed below.

C. Ultrasonics

The sound velocity $C_0(T)$ of TMH was measured at Lehigh University at 5 MHz and 15 MHz in the range 240–300 K. A linear fit to the 5-MHz data gave $C_0(T) = 2474$

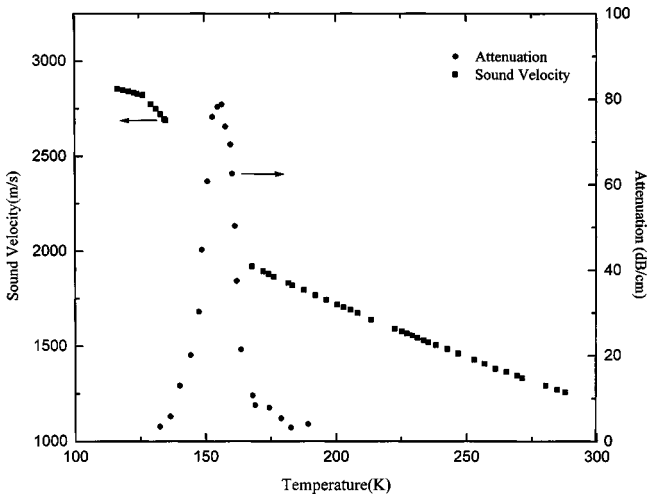

FIG. 4. Temperature dependence of the sound speed $C(T)$ determined by pulse-echo measurements at 4 MHz (■); sound attenuation in TMH at 4.4 MHz measured by an acousto-optical diffraction technique (●).

-4.4 $[T(\mathrm{K})]$ m/s (1185 m/s at 293 K). Measurements performed at the Universite P. et M. Curie in Paris at 4 MHz with the pulse-echo method gave $C_0(T)=2627$ -5.0 $[T(\mathrm{K})]$ m/s (1207 m/s at 293 K), slightly higher than the Lehigh value. As shown in Fig. 4, the pulse-echo signal disappears between 135 K and 165 K due to the high attenuation in this region. There is also a slope change near 125 K indicative of the glass transition.

In another experiment in Paris an acousto-optical diffraction technique at 4.4 MHz [3] was used to measure the attenuation in the range 132–189 K where it is between 3.5 and 79 dB/cm. (This method is very accurate for high attenuation, but is less accurate for attenuation <10 dB/cm.) As shown in Fig. 4, the maximum attenuation (where $\omega\tau\sim 1$) occurs at ~ 157 K, so that τ_{US} (157 K)~ 36 ns. (This τ_{US} point is included in Fig. 3.)

D. Brillouin scattering

Brillouin scattering experiments were carried out at City College of New York with a Sandercock tandem Fabry-Perot interferometer in six-pass (3×2) configuration with a mirror spacing of 8 mm (18.75 GHz free spectral range). The mirror reflectivity was 92%, which gave a finesse $f>60$. The 488-nm exciting light was obtained from a Coherent Innova 90 Argon laser operating in single mode.

Polarized (VV) and depolarized (VH) Brillouin spectra were collected at $\theta=90°$. The optical bandwidth was limited to 10 nm by an Amici prism–spatial filter combination. (For the depolarized backscattering experiments described below, a narrow-band interference filter was added.)

Figure 5 shows VV polarized spectra at temperatures from 294 K to 96 K with fits using the simplest version of the Mountain theory with exponential relaxation of the longitudinal viscosity [4]. In these fits, q was fixed but all other parameters—including the thermal diffusion constant—were treated as free fitting parameters since no independently determined values were available. Figure 6 shows the VV and VH spectra at 160 K on a semilogarithmic plot, demonstrating that the VH intensity is negligible compared to the VV

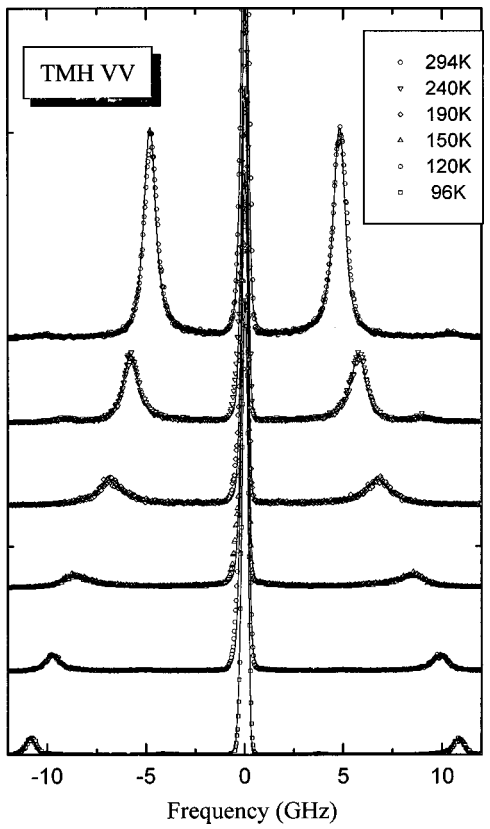

FIG. 5. VV $\theta=90°$ polarized Brillouin scattering spectra of TMH at temperatures between 294 K (top) and 96 K (bottom) with fits using the Mountain theory.

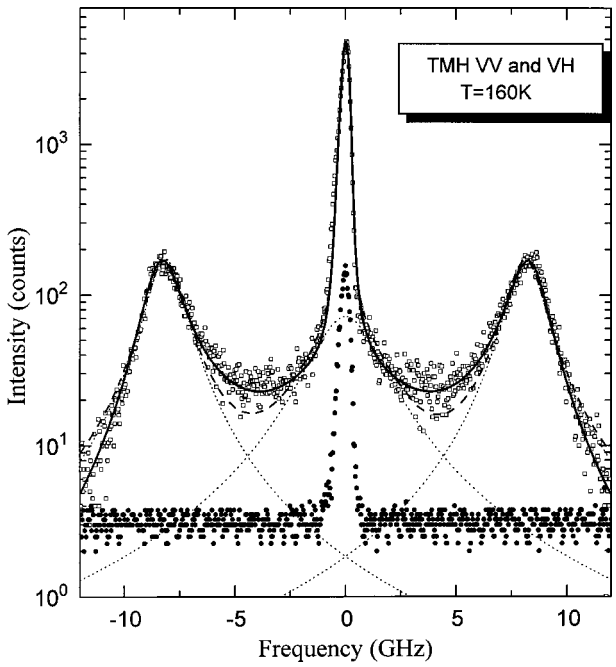

FIG. 6. VV (■) and VH (●) $\theta=90°$ Brillouin spectra of TMH at $T=160$ K. The solid line is a fit using the Mountain theory. The dashed line is a four-Lorentzian fit for which the Brillouin and Mountain components are shown separately.

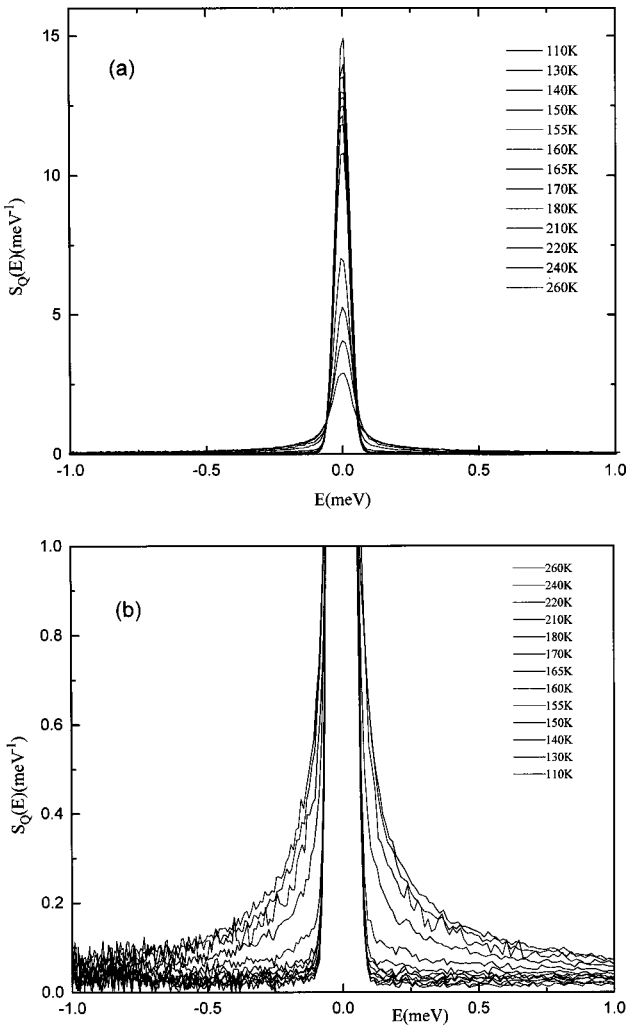

FIG. 7. $S_Q(E)$ of TMH at temperatures between 300 K and 110 K obtained by neutron-scattering time-of-flight spectroscopy. The data are shown on different vertical scales in (a) and (b). Those spectra represent an average over Q values between 0.2 and 1.7 Å^{-1}.

intensity as previously reported by Carroll and Patterson [1]. The figure shows the Mountain fit and also a separate four-Lorentzian fit with the Brillouin and Mountain modes shown separately.

E. Neutron scattering

Incoherent neutron-scattering measurements were performed on the TOF2 time of flight spectrometer at the National Institute of Standards and Technology in Gaithersburg, Maryland. The wavelength of the neutrons used was 4.8 Å, giving a resolution of approximately 60 μeV. The detection part of the spectrometer consisted of 64 detectors arranged in a circle and covering angles from 1.6° to 138.5° or, for the elastic line, wave vectors from 0.2 to 1.7 Å^{-1}. The sample was contained in a cell composed of 16 small thin-walled silica quartz tubes 1.2 mm in diameter, arranged in a plane.

The plane of the sample was oriented at 45° relative to the incident beam giving a ''dead angle'' corresponding to wave vectors 0.9–1.0 Å^{-1}, i.e. well away from the two maxima of the static structure factor at 1.5 and 1.7 Å^{-1}.

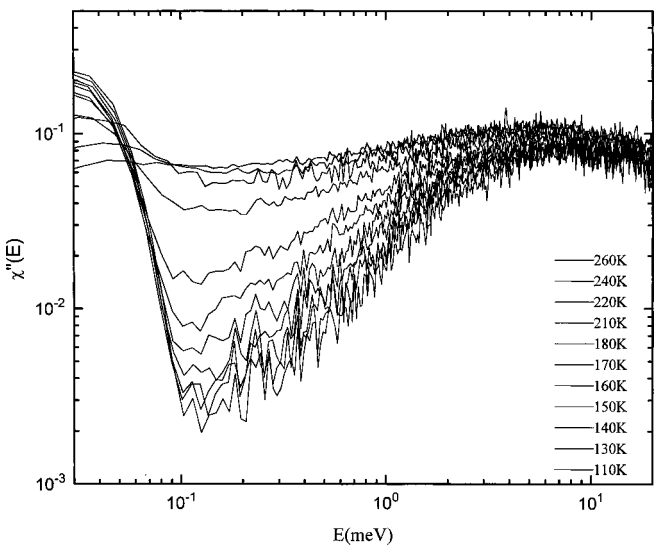

FIG. 8. Susceptibility spectra $\chi''(E)$ of TMH obtained from the neutron-scattering spectra of Fig. 7.

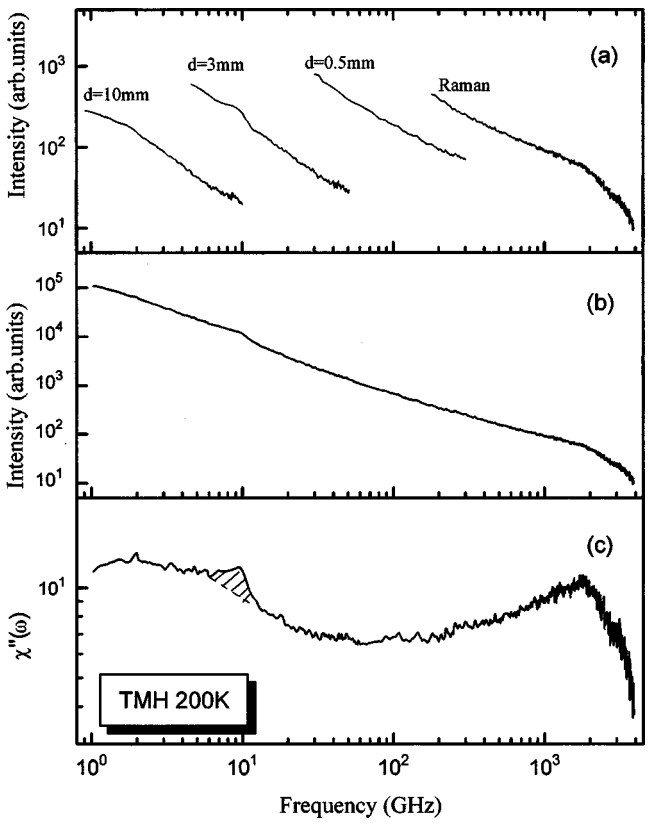

FIG. 9. Depolarized backscattering spectra of TMH at $T=200$ K. (a) Tandem Fabry-Perot spectra with $d=0.5$, 3.0, and 10.0 mm and the Raman spectrum, plotted separately. (b) The four spectra of (a) spliced to form a single composite intensity spectrum $I(\omega)$. (c) Susceptibility spectrum found from (b) with $\chi''(\omega)=I(\omega)/[n(\omega)+1]$. A 1-nm narrow-band dielectric filter was used for the spectra with $d=10$ mm and 3 mm. For the $d=0.5$ mm spectra no filter was used except for the Amici prism. The shaded region in (c) indicates leakage of the intense LA Brillouin line.

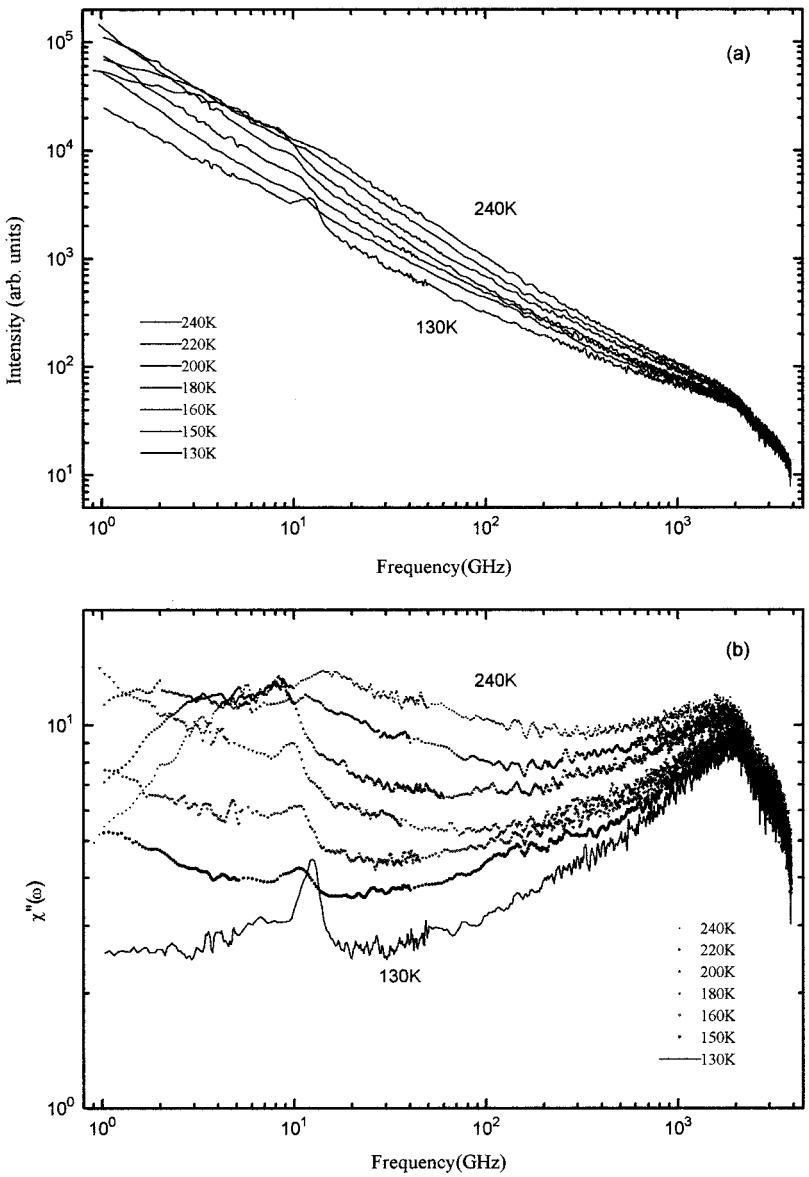

FIG. 10. Composite depolarized backscattering spectra $I(\omega)$ (a) and susceptibility spectra $\chi''(\omega)$ (b) for temperatures from 240 K to 130 K.

The resulting spectra were averaged over all the detectors and therefore represent an average over a large range of Q values. In principle, single-detector spectra could provide data at specific Q values, but the signal-to-noise ratio was too low to allow us to analyze single-detector data.

The quasielastic Q-averaged dynamical structure factor $S_Q(E)$ (centered at zero energy) is presented in Fig. 7 on two different vertical scales in order to show (a) the full elastic peaks and (b) the quasielastic tails. These tails completely vanish below 150 K, which roughly corresponds to the ideal glass transition (or crossover) temperature, T_C, determined from depolarized light scattering experiments to be discussed below. The same data are presented in Fig. 8 as a generalized susceptibility $\chi''(E)$ computed from $S_Q(E)$ by division by the Bose factor $[1+n(E)]$. This figure clearly reveals the resolution cutoff of the spectrometer at ~ 60 μeV where the resolution-broadened elastic peaks merge. At higher energies, two features are identifiable for $T \geqslant 210$ K: a weak α peak at the higher temperatures and the β minimum, both shifting towards lower energy with decreasing temperature. The neutron α peak is not very prominent, and is closer in magnitude to the α peak measured in light scattering than was the case for salol [5]. In salol, a strong contribution from rotations significantly enhanced the light-scattering α peak relative to its neutron-scattering counterpart. This suggests that, in TMH, rotations do not contribute significantly to the light scattering, which would be consistent with the low optical depolarization ratio and the apparent near-spherical conformation of the TMH molecule.

F. Depolarized light-scattering spectroscopy

In depolarized backscattering spectroscopy, first-order scattering from longitudinal (LA) and transverse (TA) modes is forbidden by symmetry. The observed spectra $I_{VH}^{180}(\omega)$ arise from a combination of orientational dynamics (for optically anisotropic molecules) and interaction-induced scattering that can be viewed as a second-order light-scattering process [6]. While for anisotropic materials such as salol the orientational scattering mechanism appears to be dominant [7], the low integrated depolarization ratio observed for TMH indicates that, for this material, orientational scattering should not be important [8]. The spectra should primarily

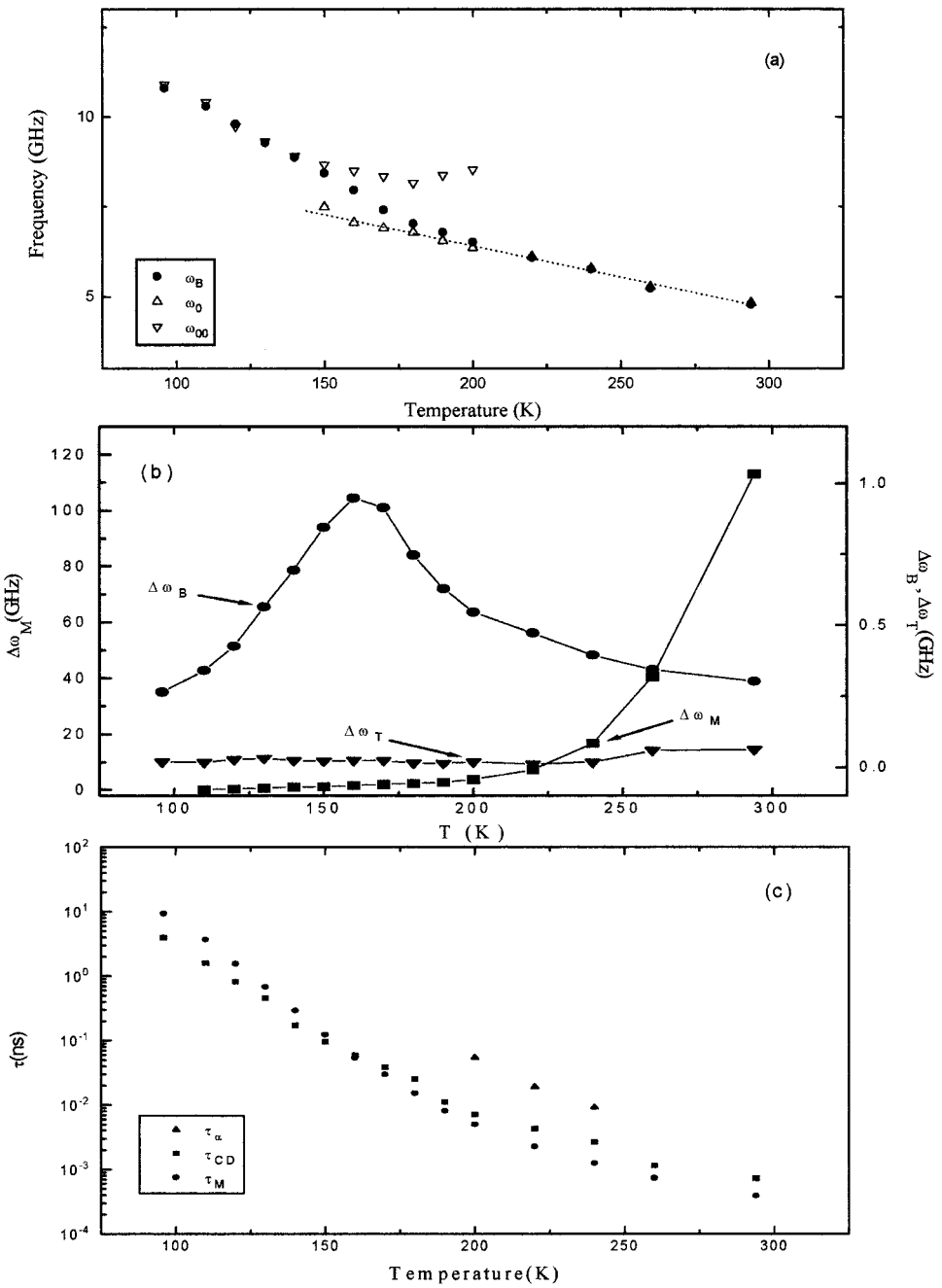

FIG. 11. Temperature dependence of (a) Brillouin peak frequency ω_B (●), low-frequency limit $\omega_0 = C_0 q$ (△) from ultrasonic measurements, and high-frequency limit $\omega_\infty = [\omega^2 + \Delta^2]^{1/2}$ (▽), from fits to Eq. (5). (b) Linewidths of the Brillouin lines ($\Delta\omega_B$) (●), Mountain mode ($\Delta\omega_M$)(■), and central thermal-diffusion mode ($\Delta\omega_T$)(▼) vs T from four-Lorentzian fits to the polarized Brillouin spectra. (c) Relaxation time τ_B from Mountain theory fits with exponential relaxation (τ_M)(●), and generalized hydrodynamics fits with the Cole-Davidson relaxation function (τ_{CD})(■) vs T. The α-relaxation time τ_α (▲) found from Kohlrausch fits to the α-peak in the depolarized $\chi''(\omega)$ spectra is also shown.

reflect the dynamics of density fluctuations and should therefore be useful for comparison with predictions of the mode-coupling theory (MCT) [9].

A preliminary depolarized light-scattering study of TMH in a limited temperature range was reported by Hwang *et al.* [8]. However, it was subsequently found that the instrumentation used in that experiment allowed some higher-order transmission of the tandem Fabry-Perot interferometer to be included in the measured spectra, causing possible distortion of the spectra at low frequencies [10]. We have therefore carried out a new set of experiments with the addition of a 1-nm narrow-bandwidth dielectric filter to suppress higher-order transmission. Unfortunately, the maximum transmission of the filter is only 30%, which, for a weak scatterer like TMH, results in a serious signal-to-noise problem. We ran many of the experiments for up to 10 h for a single spectrum in order to collect spectra with sufficient signal-to-noise levels for the analysis, but the spectra were still quite weak.

The experiments were carried out in near-backscattering geometry ($\theta = 173°$) with ~200 mW of 488-nm laser light incident on the sample. Spectra were collected with the Sandercock tandem Fabry-Perot interferometer with mirror spacings of 0.5, 3.0, and 10.0 mm and also with a Spex 1401 Raman spectrometer. The four spectra for each temperature were then spliced together to provide a single broad-frequency-range spectrum $I(\omega)$, which was then converted to a susceptibility spectrum $\chi''(\omega)$ by division by the Bose factor $[n(\omega)+1]$. Figure 9 for $T = 200$ K shows the four individual spectra (a), the single composite $I(\omega)$ spectrum (b), and the corresponding susceptibility spectrum $\chi''(\omega)$ (c). Figure 10 shows the full set of $I(\omega)$ and $\chi''(\omega)$ spectra obtained with this procedure for temperatures from 130 K to 240 K. We note that the α-peak intensity is comparable to that of the boson peak at ~2000 GHz. This is in contrast to

materials with pronounced optical anisotropy such as salol that have far stronger α peaks. In this sense TMH resembles calcium potassium nitrate for which orientational dynamics also do not contribute significantly to the light-scattering spectrum.

III. DATA ANALYSIS

A. Brillouin scattering

The VV polarized Brillouin spectra shown in Fig. 5 were first analyzed with the Mountain theory as illustrated in Fig. 6. We also followed a generalized hydrodynamics approach with

$$I(\omega)=(I_0/\omega)Im[\omega_0^2-\omega^2-i\omega\gamma_0-\omega m(\omega)]^{-1} \quad (5a)$$

with $m(\omega)$ aproximated by the Cole-Davidson relaxation function

$$\omega m(\omega)=\Delta^2[(1-i\omega\tau)^{-\beta}-1]. \quad (5b)$$

The relaxation time τ_B for longitudinal sound waves, taken either as τ_{CD} obtained from the fits to Eq. (5) or τ_M obtained with the Mountain theory (with exponential relaxation) are plotted in Fig. 11(c). We also show the α-relaxation time τ_α determined from the α peaks in the depolarized backscattering spectra of Fig. 10(b). Note that τ_α is five to ten times longer than the relaxation times τ_B inferred from the Brillouin spectra using either the generalized hydrodynamics or Mountain theories.

At temperatures below ~ 160 K where the Brillouin linewidth $\Delta\omega_B$ in Fig. 11(b) is a maximum ($\omega_B\tau_B\sim 1$), the relaxation times τ_B found in such ''α-relaxation-only'' fits to Brillouin spectra are expected to increase too slowly with decreasing T because of the increasing contributions of the fast relaxation processes that are not included [11]. This strong low-temperature disagreement is clearly seen for $T<160$ K in Fig. 3 where τ_B falls increasingly farther below all the other τ values. For $T>160$ K, however, the α-relaxation-only model should be adequate. Nevertheless, for $T=200$, 220, and 240 K, as shown in Fig. 11(c), τ_B (taken as either τ_{CD} or τ_M) is still well below τ_α found from depolarized backscattering spectra. The disagreement can also be inferred from Fig. 15 where the α peak of the depolarized backscattering spectrum at $\omega_\alpha\sim 1/\tau_\alpha$ passes through the Brillouin line at ~ 240 K while the corresponding coincidence for ω_B would occur ~ 160 K when $\tau\omega_B\sim 1$ and the Brillouin linewidth is a maximum.

Similar differences have been observed with other materials including salol, propylene carbonate, and orthoterphenyl, and have sometimes been interpreted as indicating that the α peak at $\omega_\alpha=1/\tau_\alpha$ in the depolarized spectra results primarily from orientational structural relaxation while the damping of the Brillouin modes results primarily from translational structural relaxation processes for which the α peak is at $\omega_B^\alpha=1/\tau_B$. However, since the apparent isotropy of TMH indicates that orientational dynamics should not be significant, this explanation does not appear to be relevant for TMH.

Since for TMH, the nearly isotropic structure implies that both the α peak in the depolarized spectrum and the damping of the Brillouin LA modes are due to translational structural relaxation, the disagreement between τ_α and τ_B must have an origin involving neither orientational dynamics nor fast relaxation. One possible explanation is that the Brillouin spectrum measures $S_q(\omega)$ for a well-defined (small) q value since the Brillouin scattering process is first-order allowed. So the damping of the Brillouin mode represents the relaxation dynamics of the longitudinal viscosity at the scattering wave vector q. For the depolarized backscattering geometry, on the contrary, since first-order scattering from either longitudinal or transverse modes is forbidden, scattering occurs as a second-order process from pairs of modes S_{q_1} and S_{q_2} where $q_1+q_2=q$ [6]. Since τ_α is generally a q-dependent quantity, the convolution of $S_{q_1}(\omega)$ and $S_{q_2}(\omega)$ underlying the depolarized backscatering spectrum may therefore have a different α-peak position than that of $S_q(\omega)$.

TABLE II. Parameters obtained from fits of the neutron scattering susceptibility spectra to Eq. (6).

T	a	b	χ''_{min}	ω_{min} (GHz)
260	0.266	0.741	72.7	59.3
240	0.312	1.04	61.5	51.3
220	0.381	1.26	53.5	50.2
210	0.447	1.28	36.5	35.6

B. Neutron scattering

The neutron scattering spectra $S_Q(E)$, shown in Fig. 7, were integrated between the energies corresponding to $\pm\omega_{min}$, where ω_{min} is the position of the minimum in the light-scattering susceptibility spectrum, in order to estimate the Debye-Waller factor $f_Q(T)$. The result is shown in Fig. 12 and suggests the possible presence of a cusp at ~ 150 K. The values of $f_Q(T)$ were found by dividing the intensity between $\pm\omega_{min}$ by the total intensity, which was measured separately. We note that the spectra were not corrected for elastic scattering, so that the absolute values of $f_Q(T)$ shown in Fig. 12 may be too high.

The neutron $\chi''(\omega)$ spectra of Fig. 8 were fit to the interpolation equation of MCT

$$\chi''(\omega)=\frac{\chi_{min}}{a+b}\left[a\left(\frac{\omega}{\omega_{min}}\right)^{-b}+b\left(\frac{\omega}{\omega_{min}}\right)^{a}\right] \quad (6)$$

with a and b free. The fits, in the frequency range 20–300 GHz, are shown in Fig. 13. The resulting fit parameters are given in Table II. The frequency of the minimum ω_{min} at each temperature is plotted in Fig. 14 together with the values found from the light scattering spectra.

We consider this analysis as very preliminary since, for $T\lesssim 210$ K the neutron scattering susceptibility minimum is cut off by the spectrometer resolution. The MCT analysis is therefore restricted to a temperature range well above the inferred T_C where the asymptotic analysis may no longer be valid. However, we believe that the data do establish the result that $\omega_{min}(\text{neutron})<\omega_{min}(\text{light})$ at high T. This is similar to the result obtained for salol [5]. As for salol, the two values may become equal close to T_C, but this possibility could not be studied in this preliminary experiment.

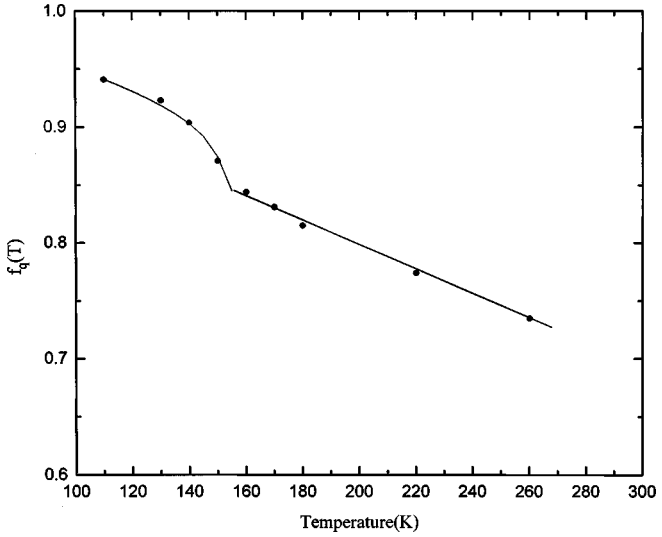

FIG. 12. Debye-Waller factor $f_Q(T)$ obtained from integration of the neutron-scattering spectra $S_Q(E)$ over the α-peak region. The integration range was $\pm E_{min}$, the position of the susceptibility minimum in the light-scattering data. The data were not corrected for elastic scattering which may make the absolute value of $f_q(T)$ too big but should not affect its qualitative temperature dependence.

C. Depolarized backscattering

The susceptibility spectra $\chi''(\omega)$ of Fig. 10(b) obtained from the depolarized backscattering spectra were analyzed by fitting the region of the susceptibility minimum (the β region) with the MCT interpolation equation (6), with a and b constrained by the MCT Γ-function relation

$$\Gamma^2(1-a)/\Gamma(1-2a)=\Gamma^2(1+b)/\Gamma(1+2b). \qquad (7)$$

The fits for $T=240$, 220, 200, 180, and 160 K were done globally, giving $a=0.268$. A separate fit for $T=150$ K gave $a=0.253$.

For the three highest temperatures, the α peak was fit with a Kohlrausch function. The fit range was varied until the theoretical α peak joined smoothly onto the MCT β fit [12].

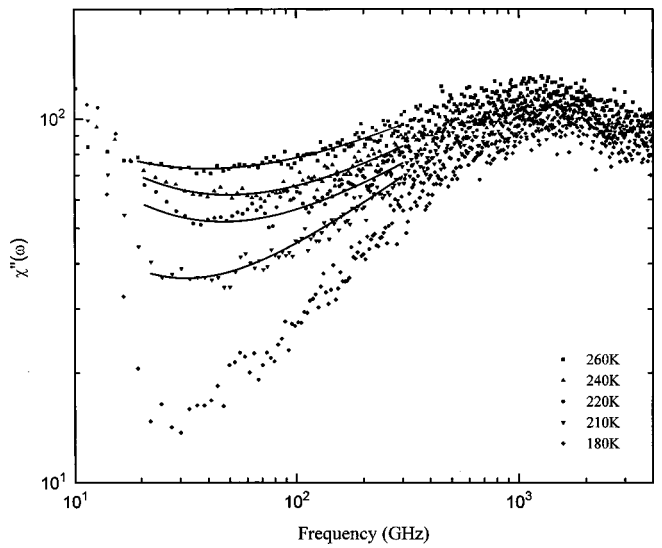

FIG. 13. Fits of neutron scattering susceptibility spectra to the interpolation equation (6) of MCT with a and b free.

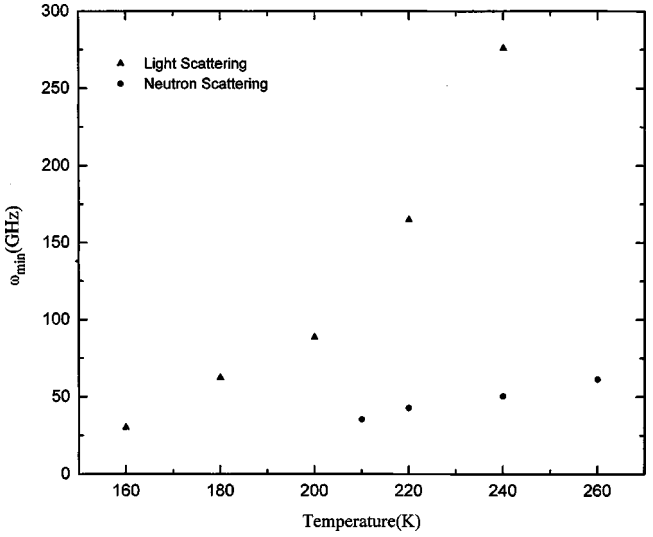

FIG. 14. Position of the susceptibility minimum ω_{min} found from light scattering (▲) and neutron scattering spectra (●).

The combined α-β fits with $\beta_K\sim 0.78$ for $T=240$, 220, and 200 K, and the β fits for $T=180$, 160, and 150 K are shown in Fig. 15.

The lowest temperature $\chi''(\omega)$ spectrum shown in Fig. 15 is at 130 K, 20 K below our estimated $T_C\sim 150$ K. In contrast to other materials studied by this technique, however, the low-frequency region at 130 K appears nearly flat rather than exhibiting the usual positive slope. This result may indicate the presence of an additional weak low-frequency scattering mechanism, but the spectrum is too weak at this temperature to merit further analysis.

The susceptibility minimum χ''_{min} is predicted by MCT to obey

$$(\chi''_{min})^2 \propto (T-T_C). \qquad (8)$$

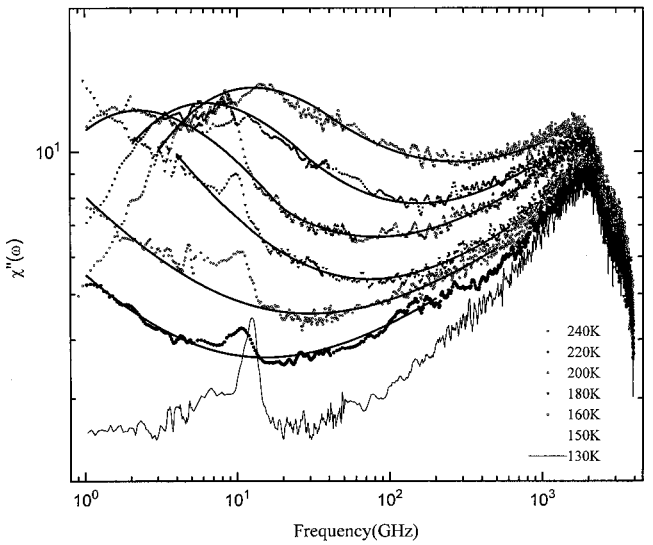

FIG. 15. Fits of the depolarized backscattering spectra of Fig. 10 to the MCT interpolation equation (6) for the β region and also, for $T=240$, 220 and 200 K, to a Kohlrausch function with $\beta_K\sim 0.78$ in the α-peak region. The α fit range was adjusted to provide a smooth match to the β fit. The resulting τ values are shown in Fig. 3 as τ_α.

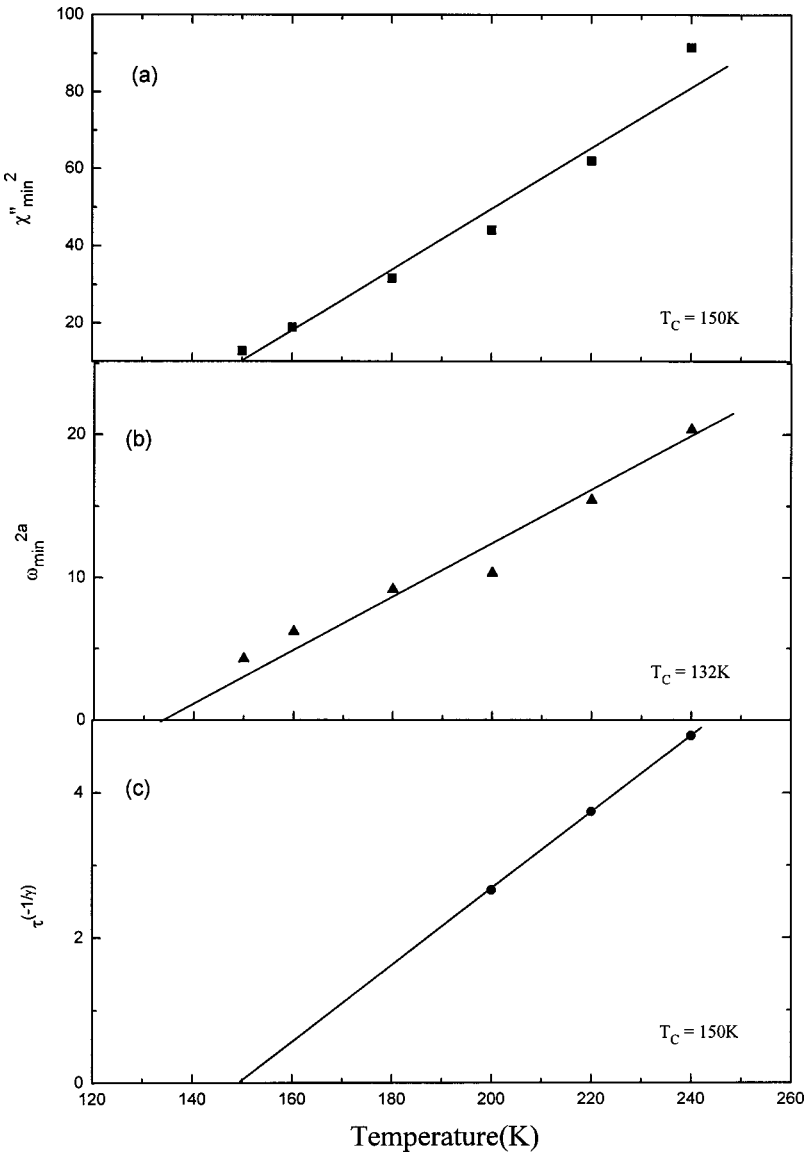

FIG. 16. (a) $(\chi''_{min})^2$ vs T found from the MCT fits of Fig. 15. A linear fit gives $T_C \sim 150$ K. (b) ω^{2a}_{min} vs T from the MCT fits of Fig. 15. (c) $\tau^{-1/\gamma}$ vs T deduced from Kohlrausch fits to the α peaks in Fig. 15 for $T=240$, 220, and 200 K. A liner fit gives $T_C \sim 150$ K.

As shown in Fig. 16(a), a plot of $(\chi''_{min})^2$ vs T is roughly linear and extrapolates to zero at approximately 150 K, providing another estimate of T_C. MCT also predicts that

$$\omega^{2a}_{min} \propto (T - T_C). \tag{9}$$

However, a plot of ω^{2a}_{min} vs T, shown in Fig. 16(b) has excessive scatter, and a linear fit extrapolated to zero at ~ 130 K, a value we consider too low to be T_C.

For the relaxation time τ_α of the α peak, MCT predicts that

$$\tau_\alpha^{-1/\gamma} \propto (T - T_C). \tag{10}$$

A plot of $\tau_\alpha^{-1/\gamma}$ vs T is shown in Fig. 16(c). Although there are only three points, a linear fit is possible and indicates an intercept ~ 150 K in agreement with the $(\chi''_{min})^2$ result of Fig. 16(a) and the cusp in $f_Q(T)$ in Fig. 12.

An unexpected observation in TMH is that the β minimum in the susceptibility obtained from neutron scattering appears at a lower frequency than the β minimum obtained from light scattering. This difference was understandable in salol because of the greater contribution of rotations to light scattering and suggested that there exist, in salol, two distinct correlators, one for rotational motion and another for translational motion [13,5]. It is, however, puzzling in TMH, in which rotations do not appear to play a major role.

IV. CONCLUSIONS

Trimethylheptane appears to have a nearly isotropic molecular structure, as evidenced by its low optical depolarization ratio and dielectric susceptibility, as well as by the structure simulation shown in Fig. 1. MCT analyses of the β-relaxation region of the neutron-scattering and light-scattering spectra nevertheless give different values for ω_{min} as shown in Fig. 14, possibly indicating that the asymptotic region in which universality applies is very narrow. Also, the values of the α-relaxation time determined from Brillouin scattering (τ_B) and depolarized light-scattering measurements (τ_α) are significantly different as shown in Fig. 3. Such differences have previously been attributed to the differing importance of orientational dynamics for different experimental techniques. The occurrence of these differences for TMH suggests that their origin is not yet understood. The

preliminary MCT analyses presented here suggest that $T_C \sim 150$ K.

Unfortunately, although trimethylheptane seems promising for the studies described here, it has a very low dielectric constant and very low depolarized light scattering intensity, making it difficult to study by dielectric and depolarized light scattering techniques. It is just the apparent molecular isotropy—the property that makes this material so interesting—that is responsible for the difficulty. Nevertheless, we conclude that the preliminary results reported here indicate that further study of this material, including extended viscosity measurements, would be highly desirable.

ACKNOWLEDGMENTS

We thank Gary Patterson for suggesting TMH to us and Craig Brown for help in the neutron-scattering experiment and for the structure analysis shown in Fig. 1. We also thank Wolfgang Götze for a careful reading of the manuscript and for many helpful suggestions. Research at CCNY was supported by the National Science Foundation under Grant No. DMR-9616577.

[1] P. J. Carroll and G. D. Patterson, J. Chem. Phys. **81**, 1666 (1984).

[2] C. L. Yaws, D. Chen, H. C. Yang, L. Tan, and D. Nico, Hydrocarbon Process. **68**, 61 (1989).

[3] C. Turc, B. Perrin, and J. B. Berger, Phys. Scr. **43**, 116 (1991).

[4] R. D. Mountain, J. Res. Natl. Bur. Stand., Sect. A **70**, 207 (1966); **72**, 95 (1968).

[5] J. Toulouse, R. Pick, and C. Dreyfus, in *Disordered Materials and Interfaces*, edited by H. E. Stanley *et al.*, MRS Symposia Proceedings No. 407 (Materials Research Society, Pittsburgh, 1996), p. 161.

[6] N. J. Tao, G. Li, X. Chen, W. M. Du, and H. Z. Cummins, Phys. Rev. A **44**, 6665 (1991), Sec. IV.

[7] H. Z. Cummins, G. Li, W. Du, R. M. Pick, and C. Dreyfus, Phys. Rev. E **53**, 896 (1996); **55**, 1232(E) (1997).

[8] Y. H. Hwang, G. Q. Shen, and H. Z. Cummins, J. Non-Cryst. Solids **235-237**, 180 (1998).

[9] For a review of MCT, see W. Götze and L. Sjogren, Rep. Prog. Phys. **55**, 241 (1992); for a recent review of experimental tests of MCT, see W. Götze, J. Phys.: Condens. Matter **11**, A1 (1999).

[10] N. V. Surovtsev, J. A. H. Wiedersich, V. N. Novikov, E. Rossler, and A. P. Sokolov, Phys. Rev. B **58**, 14 888 (1998); J. Gapinski, W. Steffen, A. Patkowski, A. P. Sokolov, A. Kisliuk, U. Buchenau, M. Russina, F. Mezei, and H. Schober, J. Chem. Phys. **110**, 2312 (1999); H. C. Barshilia, G. Li, G. Q. Shen, and H. Z. Cummins, Phys. Rev. E **59**, 5625 (1999).

[11] H. Z. Cummins, G. Li, W. M. Du, and J. Hernandez, J. Non-Cryst. Solids **172-174**, 26 (1994).

[12] H. Z. Cummins, G. Li, W. M. Du, Y. H. Hwang, and G. Q. Shen, Prog. Theor. Phys. Suppl. **126**, 21 (1997).

[13] J. Toulouse, G. Coddens, and R. Pattnaik, Physica A **201**, 305 (1993).